

High-order algorithms for solving eigenproblems over discrete surfaces

Sheng-Gwo Chen^{*,a}, Mei-Hsiu Chi^b, Jyh-Yang Wu^b

^a*Department of Applied Mathematics, National Chiayi University, Chia-Yi 600, Taiwan.*

^b*Department of Mathematics, National Chung Cheng University, Chia-Yi 621, Taiwan.*

Abstract

The eigenvalue problem of the Laplace-Beltrami operators on curved surfaces plays an essential role in the convergence analysis of the numerical simulations of some important geometric partial differential equations which involve this operator. In this note we shall combine the local tangential lifting (LTL) method with the configuration equation to develop a new effective and convergent algorithm to solve the eigenvalue problems of the Laplace-Beltrami operators acting on functions over discrete surfaces. The convergence rates of our algorithms of discrete Laplace-Beltrami operators over surfaces is $O(r^n)$, $n \geq 1$, where r represents the size of the mesh of discretization of the surface. The problem of high-order accuracies will also be discussed and used to compute geometric invariants of the underlying surfaces. Some convergence tests and eigenvalue computations on the sphere, tori and a dumbbell are presented.

Key words: Eigenproblem, Local tangential lifting method, Configuration equation, Discrete Laplace-Beltrami operator.

1. Introduction

Let Σ be a smooth regular surface in the 3D space. The Laplace-Beltrami (LB) operator is a natural generalization of the classical Laplacian Δ_Σ from the Euclidean space to a curved space. To understand the LB operators on curved surfaces, it is natural to investigate their associated eigenvalue problems:

$$\Delta_\Sigma \phi = \lambda \phi. \quad (1)$$

Or, more generally,

$$\nabla_\Sigma \cdot (h \nabla_\Sigma \phi) = \lambda \phi \quad (2)$$

where h is C^2 real function on Σ .

*Corresponding author email : csg@mail.nyu.edu.tw

Email addresses: mhchi@math.ccu.edu.tw (Mei-Hsiu Chi), jyw@math.ccu.edu.tw (Jyh-Yang Wu)

The eigenvalue problem of the LB operator plays important roles not just in the study of geometric properties of curved spaces, but also in many applications in the fields of physics, engineering and computer science. The LB operator has recently many applications in a variety of different areas, such as surface processing[6, 14], signal processing[12] and geometric partial differential equations[7].

Since the objective underlying surfaces to be considered are usually represented as discrete meshes in these applications, it is useful in practice to discretize the LB operators and solving the eigenproblems over discrete surfaces. There are many approaches for estimating Laplace-Beltrami operator and solving the Laplace-Beltrami eigenproblems [16, 17]. In 2011, Macdonald[10] proposed an elegant method to solve the Laplace-Beltrami eigenproblems for Equations (1) and (2) by the closest point method[13]. In this paper we shall describe simple and effective methods with high-order accuracies to define the discrete LB operator on functions on a triangular mesh.

In 2012, Ray et al.[15] used the method of least square to obtain high-order approximations of derivatives and integrations. In this paper, we shall use ideas developed in Chen, Chi and Wu[3, 4] where we try to estimate the discrete partial derivatives of functions on 2D scattered data points. Indeed, the ideas that we shall use to develop our algorithms are divided into two main steps: first we lift the 1-neighborhood points to the approximating tangent space and obtain a local tangential polygon. Second, we use some geometric idea to lift functions to the tangent space. We call this a local tangential lifting (LTL) method[5, 19]. Then we present a new algorithm, the configuration method, to compute their Laplacians in the 2D tangent space. This means that the LTL process allows us to reduce the 2D curved surface problem to the 2D Euclidean problem.

In other words, we shall combine the local tangential lifting (LTL) method with the configuration equation to develop a new effective and convergent algorithm to solve the eigenpair problems of the Laplace-Beltrami operators acting on functions over curved surfaces. We shall also present a mathematical proof of the convergence of our algorithm. Our algorithm is not only conceptually simple, but also easy to implement. Indeed, the convergence rate of our new algorithms of discrete Laplace-Beltrami operators over surfaces is $O(r^n)$, $n \geq 1$, where r represents the size of the mesh of discretization of the surface. In section 2, we introduce the gradient of a function, the divergence of a vector field and the Laplace-Beltrami operator on regular surfaces. Our $O(r)$ -LTL configuration method is discussed in section 3. In section 4, we discuss how to improve the methods to have high-order accuracies. We also give some numerical simulations to support these results in section 5.

2. The gradient, divergence, and Laplace-Beltrami operator

In order to describe the gradient, divergence and the LB operator on functions or vector fields in a regular surface Σ in the 3D Euclidean space \mathbb{R}^3 , we consider a parameterization $\mathbf{x} : U \rightarrow \Sigma$ at a point \mathbf{p} , where U is an open subset of

the 2D Euclidean space \mathbb{R}^2 . We can choose, at each point \mathbf{q} of $\mathbf{x}(U)$, a unit normal vector $\mathbf{N}(\mathbf{q})$. The map $\mathbf{N} : \mathbf{x}(U) \rightarrow \mathbb{S}^2$ is the local Gauss map from an open subset of the regular surface Σ to the unit sphere \mathbb{S}^2 in the 3D Euclidean space \mathbb{R}^3 . Denote the tangent space of Σ at the point \mathbf{p} by $T\Sigma_{\mathbf{p}} = \{\mathbf{v} \in \mathbb{R}^3 | \mathbf{v} \perp \mathbf{N}(\mathbf{p})\}$. The tangent space $T\Sigma_{\mathbf{p}}$ is a linear space spanned by $\{\mathbf{x}_u, \mathbf{x}_v\}$ where u, v are coordinates for U .

The gradient $\nabla_{\Sigma}g$ of a smooth function g on Σ can be computed from

$$\nabla_{\Sigma}g = \frac{g_u G - g_v F}{EG - F^2} \mathbf{x}_u + \frac{g_v E - g_u F}{EG - F^2} \mathbf{x}_v \quad (3)$$

where E, F , and G are the coefficients of the first fundamental form and

$$g_u = \frac{\partial g(\mathbf{x}(u, v))}{\partial u} \text{ and } g_v = \frac{\partial g(\mathbf{x}(u, v))}{\partial v}. \quad (4)$$

See do Carmo[8, 9] for the details.

Let $\mathbf{X} = A\mathbf{x}_u + B\mathbf{x}_v$ be a local vector field on Σ . The divergence, $\nabla_{\Sigma} \cdot \mathbf{X}$, of \mathbf{X} is defined as a function $\nabla_{\Sigma} \cdot \mathbf{X} : \Sigma \rightarrow \mathbb{R}$ given by the trace of the linear mapping $\mathbf{Y}(\mathbf{p}) \rightarrow \nabla_{\mathbf{Y}(\mathbf{p})}\mathbf{X}$ for $\mathbf{p} \in \Sigma$. A direct computation gives

$$\nabla_{\Sigma} \cdot X = \frac{1}{\sqrt{EG - F^2}} \left(\frac{\partial}{\partial u} (A\sqrt{EG - F^2}) + \frac{\partial}{\partial v} (B\sqrt{EG - F^2}) \right). \quad (5)$$

The LB operator acting on the function g is defined by

$$\Delta_{\Sigma}g = \nabla_{\Sigma} \cdot \nabla_{\Sigma}g. \quad (6)$$

for all smooth function g on Σ . A direct computation yields the following local representation for the LB operator on a smooth function g :

$$\begin{aligned} \Delta_{\Sigma}g = & \frac{1}{\sqrt{EG - F^2}} \left[\frac{\partial}{\partial u} \left(\frac{G}{\sqrt{EG - F^2}} \frac{\partial g}{\partial u} \right) - \frac{\partial}{\partial u} \left(\frac{F}{\sqrt{EG - F^2}} \frac{\partial g}{\partial v} \right) \right] \\ & + \frac{1}{\sqrt{EG - F^2}} \left[\frac{\partial}{\partial v} \left(\frac{E}{\sqrt{EG - F^2}} \frac{\partial g}{\partial v} \right) - \frac{\partial}{\partial v} \left(\frac{F}{\sqrt{EG - F^2}} \frac{\partial g}{\partial u} \right) \right]. \end{aligned} \quad (7)$$

3. An $O(r)$ -LTL configuration method

In this section, we shall introduce a new algorithm to solve the eigenpair problems, Equations (1) and (2), by the LTL configuration method.

Consider a triangular surface mesh $S = (V, F)$, where $V = \{\mathbf{v}_i | 1 \leq i \leq n_V\}$ is the list of vertices and $F = \{T_k | 1 \leq k \leq n_F\}$ is the list of triangles.

To describe the local tangential lifting (LTL) method, we introduce the approximating tangent plane $TS_A(\mathbf{v})$ and the local tangential polygon $P_A(\mathbf{v})$ at the vertex \mathbf{v} of S as follows:

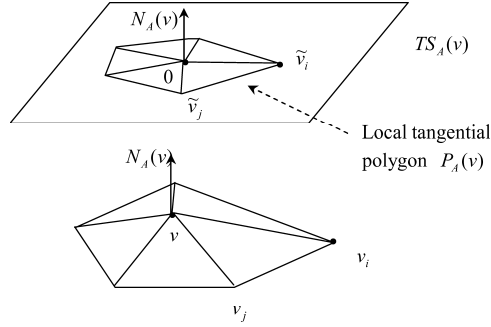


Figure 1: The local tangential polygon $P_A(\mathbf{v})$

1. The normal vector $\mathbf{N}_A(\mathbf{v})$ at the vertex \mathbf{v} in S is given by

$$\mathbf{N}_A(\mathbf{v}) = \frac{\sum_{T \in T(\mathbf{v})} \omega_T \mathbf{N}_T}{\|\sum_{T \in T(\mathbf{v})} \omega_T \mathbf{N}_T\|} \quad (8)$$

where $T(\mathbf{v})$ is the set of triangles that contain the vertex \mathbf{v} , \mathbf{N}_T is the unit normal to a triangle face T with $\langle \mathbf{N}_T, \mathbf{N}'_T \rangle > 0$ for all $T, T' \in T(\mathbf{v})$ and the centroid weight is given in [1, 2] by

$$\omega_T = \frac{\frac{1}{\|\mathbf{G}_T - \mathbf{v}\|^2}}{\sum_{\tilde{T} \in T(\mathbf{v})} \frac{1}{\|\mathbf{G}_{\tilde{T}} - \mathbf{v}\|^2}} \quad (9)$$

where \mathbf{G}_T is the centroid of the triangle face T determined by

$$\mathbf{G}_T = \frac{\mathbf{v} + \mathbf{v}_i + \mathbf{v}_j}{3}. \quad (10)$$

Note that the letter A in the notation $\mathbf{N}_A(v)$ stands for the word "Approximation".

2. The approximating tangent plane $TS_A(\mathbf{v})$ of S at \mathbf{v} is now determined by $TS_A(\mathbf{v}) = \{\mathbf{w} \in \mathbb{R}^3 \mid \mathbf{w} \perp \mathbf{N}_A(\mathbf{v})\}$.
3. The local tangential polygon $P_A(\mathbf{v})$ of \mathbf{v} in $TS_A(\mathbf{v})$ is formed by the vertices $\bar{\mathbf{v}}_i$ which is the lifting vertex of \mathbf{v}_i adjacent to \mathbf{v} in V :

$$\bar{\mathbf{v}}_i = (\mathbf{v}_i - \mathbf{v}) - \langle \mathbf{v}_i - \mathbf{v}, \mathbf{N}_A(\mathbf{v}) \rangle \mathbf{N}_A(\mathbf{v}) \quad (11)$$

as in figure 1.

4. We can choose an orthonormal basis $\mathbf{e}_1, \mathbf{e}_2$ for the tangent plane $TS_A(\mathbf{v})$ of S at \mathbf{v} and obtain an orthonormal coordinates (x, y) for vectors $\mathbf{w} \in TS_A(\mathbf{v})$ by $\mathbf{w} = x\mathbf{e}_1 + y\mathbf{e}_2$. We set $\bar{\mathbf{v}}_i = x_i\mathbf{e}_1 + y_i\mathbf{e}_2$ with respect to the orthonormal basis $\mathbf{e}_1, \mathbf{e}_2$.

Now we explain how to lift locally a function defined on V to the local tangential polygon $P_A(\mathbf{v})$. Consider a function ϕ on V . We will lift locally the

function ϕ to a function of two variables, denoted by $\bar{\phi}$, on the vertices $\bar{\mathbf{v}}_i$ in $P_A(\mathbf{v})$ by simply setting

$$\bar{\phi}(x_i, y_i) = \phi(\mathbf{v}_i) \quad (12)$$

and $\bar{\phi}(\vec{0}) = \phi(\mathbf{v})$ where $\vec{0}$ is the origin of $TS_A(\mathbf{v})$. Then one can extend the function $\bar{\phi}$ to be a piecewise linear function on the whole polygon $P_A(\mathbf{v})$ in a natural and obvious way.

Next, we introduce the configuration matrices for $\Delta_\Sigma \phi$ and $\nabla_\Sigma \cdot (h \nabla_\Sigma \phi)$ in Equations (1) and (2).

3.1. The Configuration matrix for $\Delta_\Sigma \phi$

According to the LTL method, the differential quantities at a point on curved surfaces correspond to planar differential quantities in \mathbb{R}^2 . Hence, we only need to estimate the Laplace-Beltrami operator on planar triangular meshes. Given a C^3 function f on an open domain $\Omega \subset \mathbb{R}^2$ with the origin $(0, 0) \in \Omega$, Taylor's expansion for two variables x and y gives

$$\begin{aligned} f(x, y) &= f(0, 0) + x f_x(0, 0) + y f_y(0, 0) \\ &\quad + \frac{x^2}{2} f_{xx}(0, 0) + xy f_{xy}(0, 0) \\ &\quad + \frac{y^2}{2} f_{yy}(0, 0) + O(r^3) \end{aligned} \quad (13)$$

when $r = x^2 + y^2$ is small.

Consider a family of neighboring points $(x_j, y_j) \in \Omega$, $j = 1, 2, \dots, n$, of the origin $(0, 0)$. Take some constants α_j , $j = 1, 2, \dots, n$, with $\sum_{j=1}^n \alpha_j = \epsilon \neq 0$. Then one has

$$\begin{aligned} &\sum_{j=1}^n \alpha_j (f(x_j, y_j) - f(0, 0)) \\ &= \left(\sum_{j=1}^n \alpha_j x_j \right) f_x(0, 0) + \left(\sum_{j=1}^n \alpha_j y_j \right) f_y(0, 0) \\ &\quad + \frac{1}{2} \left(\sum_{j=1}^n \alpha_j x_j^2 \right) f_{xx}(0, 0) + \left(\sum_{j=1}^n \alpha_j x_j y_j \right) f_{xy}(0, 0) \\ &\quad + \frac{1}{2} \left(\sum_{j=1}^n \alpha_j y_j^2 \right) f_{yy}(0, 0) + O(r^3), \end{aligned} \quad (14)$$

where $r = \max_{j \in \{1, 2, \dots, n\}} \{\sqrt{x_j^2 + y_j^2}\}$. To estimate the Laplacian, $f_{xx}(0, 0) + f_{yy}(0, 0)$, at $(0, 0)$, we choose the constants α_j , $j = 1, 2, \dots, n$ with $\sum_{j=1}^n \alpha_j = \epsilon$, so that they satisfy the following equations:

$$\sum_{j=1}^n \alpha_j x_j = 0,$$

$$\sum_{j=1}^n \alpha_j y_j = 0,$$

$$\sum_{j=1}^n \alpha_j x_j y_j = 0,$$

and

$$\sum_{j=1}^n \alpha_j x_j^2 = \sum_{j=1}^n \alpha_j y_j^2$$

or equivalently

$$\sum_{j=1}^n \alpha_j (x_j^2 - y_j^2) = 0$$

One can rewrite these equations in a matrix form with the condition $\sum_{j=1}^n \alpha_j = \epsilon$ and obtain the following equation:

$$\begin{pmatrix} x_1, & x_2, & \cdots, & x_n \\ y_1, & y_2, & \cdots, & y_n \\ x_1 y_1, & x_2 y_2, & \cdots, & x_n y_n \\ x_1^2 - y_1^2, & x_2^2 - y_2^2, & \cdots, & x_n^2 - y_n^2 \\ 1, & 1, & \cdots, & 1 \end{pmatrix} \begin{pmatrix} \alpha_1 \\ \alpha_2 \\ \vdots \\ \alpha_n \end{pmatrix} = \begin{pmatrix} 0 \\ 0 \\ 0 \\ 0 \\ \epsilon \end{pmatrix}. \quad (15)$$

The solutions α_j of this equation allow us to obtain a formula for the Laplacian $\Delta f(0, 0)$:

$$\begin{aligned} \Delta f(0, 0) &= f_{xx}(0, 0) + f_{yy}(0, 0) \\ &= \frac{2 \sum_{j=1}^n \alpha_j (f(x_j, y_j) - f(0, 0))}{\sum_{j=1}^n \alpha_j x_j^2} + O(r) \end{aligned} \quad (16)$$

Remark 1. 1. Equation (15) is called the configuration equation of the Laplace-Beltrami operator. We call the matrix $(x_i, y_i, x_i y_i, x_i^2 - y_i^2)^T$ in Equation (15) the configuration matrix of Laplace-Beltrami operator and the solution (α_i) in Equation (15) the configuration coefficients of the Laplace-Beltrami operator, respectively.

2. For the reason of symmetry, Equation (16) also gives

$$\Delta f(0, 0) = \frac{4 \sum_{j=1}^n \alpha_j (f(x_j, y_j) - f(0, 0))}{\sum_{j=1}^n \alpha_j (x_j^2 + y_j^2)} + O(r) \quad (17)$$

since we have $\sum_{j=1}^n \alpha_j x_j^2 = \sum_{j=1}^n \alpha_j y_j^2$.

3. For simplicity, the scalar ϵ in Equation (15) can be chosen to be 1.
4. It is worth to point out that Equation (17) is an generalization of the well-known 5-point Laplacian formula. In the 5-point Laplacian case, we have the origin $(0,0)$ along with 4 neighboring points $(s,0)$, $(0,s)$, $(-s,0)$ and $(0,-s)$ for sufficiently small positive number s . One can find a solution $\alpha_j = \frac{1}{4}$ for $j = 1, 2, 3, 4$, in this case.

Now, let Σ be a regular surface with a triangular surface mesh $S = (V, F)$ of Σ . The set $V = \{\mathbf{v}_i | i = 1, 2, \dots, n_V\}$ is the list of vertices on S , $F = \{T_k | k = 1, 2, \dots, n_F\}$ is the list of triangles on S and $N(i)$ is the number of 1-neighbors of \mathbf{v}_i on S . Suppose that ϕ is a C^3 function on S . For each vertex \mathbf{v}_i on S , $\{\bar{\mathbf{v}}_{i,j}\}_{j=1}^{N(i)}$ is the tangential polygon of the neighbors of \mathbf{v}_i with coordinates $\{(x_{i,j}, y_{i,j}) | i = 1, 2, \dots, N(i)\}$ and $\phi(x_{i,j}, y_{i,j}) = \phi(\mathbf{v}_{i,j})$ is the lifting function of ϕ . By the configuration equation of the Laplacian in Equation (15), the Laplace-Beltrami operator, $\Delta_S \phi$ on S , is defined by

$$\Delta_S \phi(\mathbf{v}_i) = \frac{2 \sum_{j=1}^{N(i)} \alpha_{i,j} (\phi(x_{i,j}, y_{i,j}) - \phi(0,0))}{\sum_{j=1}^{N(i)} (\alpha_{i,j} x_{i,j}^2)}. \quad (18)$$

Then one can prove

Theorem 1. *Given a smooth function ϕ on a closed regular surface Σ and a triangular surface mesh $S = (V, F)$ with mesh size r , one has*

$$\Delta_\Sigma \phi(\mathbf{v}) = \Delta_S \phi(\mathbf{v}) + O(r) \quad (19)$$

where the discrete LB operator $\Delta_S \phi(\mathbf{v})$ is given in Equation (18).

We will prove Theorem 1 by the following 4 Lemmas. Indeed, Theorems 2 and 3 in this section can also be proved in a similar way.

Given a smooth function h on a regular surface Σ , we can lift h via the exponential map $\exp_{\mathbf{p}}$ locally to obtain a smooth function \hat{h} defined on $W \in T\Sigma(\mathbf{p})$ by setting

$$\hat{h}(\mathbf{w}) = h(\exp_{\mathbf{p}}(\mathbf{w})) \quad (20)$$

for $\mathbf{w} \in W$. Fix an orthonormal basis $\tilde{\mathbf{e}}_1, \tilde{\mathbf{e}}_2$ for the tangent space $T\Sigma(\mathbf{p})$. This gives us a coordinate system on $T\Sigma(\mathbf{p})$. Namely, for $\mathbf{w} \in W$ we have $\mathbf{w} = x\tilde{\mathbf{e}}_1 + y\tilde{\mathbf{e}}_2$ for two constants x and y . Without loss of ambiguity, we can identify the vector $\mathbf{w} \in W$ with the vector (x, y) with respect to the orthonormal basis $\tilde{\mathbf{e}}_1, \tilde{\mathbf{e}}_2$. In this way, the function \hat{h} can also give us a smooth function \tilde{h} of two variables x and y by defining

$$\tilde{h}(x, y) = \hat{h}(\mathbf{w}) \quad (21)$$

for $\mathbf{w} = x\tilde{\mathbf{e}}_1 + y\tilde{\mathbf{e}}_2$. Using these notations, we will prove

Lemma 1. *One has*

$$\Delta_\Sigma h(\mathbf{p}) = \Delta \hat{h}(0) = \Delta \tilde{h}(0, 0). \quad (22)$$

Proof. It is well-known that the LB operator $\Delta_\Sigma h(\mathbf{p})$ acting on a smooth function h at a point \mathbf{p} can be computed from the second derivatives of h along any two perpendicular geodesics with unit speed. See do Carmo [9] for details. Indeed, we consider the following two perpendicular geodesics with unit speed in Σ by using the orthonormal vectors $\tilde{\mathbf{e}}_1, \tilde{\mathbf{e}}_2$:

$$c_i(t) = \exp_{\mathbf{p}}(t\tilde{\mathbf{e}}_i), \quad i = 1, 2 \quad (23)$$

with $c_i(0) = \mathbf{p}$ and $\frac{dc_i}{dt}(0) = \tilde{\mathbf{e}}_i$. One has

$$\begin{aligned} \Delta_\Sigma h(\mathbf{p}) &= \frac{d^2}{dt^2} h(c_1(t))|_{t=0} + \frac{d^2}{dt^2} h(c_2(t))|_{t=0} \\ &= \frac{d^2}{dt^2} \hat{h}(t\tilde{\mathbf{e}}_1)|_{t=0} + \frac{d^2}{dt^2} \hat{h}(t\tilde{\mathbf{e}}_2)|_{t=0} \\ &= \Delta \hat{h}(\vec{0}) \\ &= \frac{\partial^2 \tilde{h}}{\partial x^2}(0, 0) + \frac{\partial^2 \tilde{h}}{\partial y^2}(0, 0) \\ &= \Delta \tilde{h}(0, 0). \end{aligned} \quad (24)$$

□

Next we consider a triangular surface mesh $S = \{V, F\}$ for the regular surface Σ , where $V = \{v_i | 1 \leq i \leq n_V\}$ is the list of vertices and $F = \{T_k | 1 \leq k \leq n_F\}$ is the list of triangles and the mesh size is less than r . Fix a vertex \mathbf{v} in V . For each face $T \in F$ containing \mathbf{v} , we have

$$\mathbf{N}_\Sigma(\mathbf{v}) = \mathbf{N}_T + O(r) \quad (25)$$

where $\mathbf{N}_\Sigma(\mathbf{v})$ is the unit normal vector of the true tangent plane $T\Sigma(\mathbf{v})$ of Σ at \mathbf{v} and \mathbf{N}_T is the unit normal vector of the face T . Since the approximating normal vector $\mathbf{N}_A(\mathbf{v})$, defined in section 3 is a weighted sum of these neighboring face normals \mathbf{N}_T , we have

Lemma 2. *One has*

$$\mathbf{N}_\Sigma(\mathbf{v}) = \mathbf{N}_A \mathbf{v} + O(r). \quad (26)$$

Due to this lemma, the orthonormal basis $\tilde{\mathbf{e}}_1, \tilde{\mathbf{e}}_2$ for the tangent plane $T\Sigma(\mathbf{v})$ will give us an orthonormal basis $\mathbf{e}_1, \mathbf{e}_2$ for the approximating tangent space $T\Sigma_A(\mathbf{v}) = \{\mathbf{w} \in \mathbb{R}^3 | \mathbf{w} \perp \mathbf{N}_A(\mathbf{v})\}$ by the Gram-Schmidt process in linear algebra:

$$\mathbf{e}_1 = \frac{\tilde{\mathbf{e}}_1 - \langle \tilde{\mathbf{e}}_1, \mathbf{N}_A(\mathbf{v}) \rangle \mathbf{N}_A(\mathbf{v})}{\|\tilde{\mathbf{e}}_1 - \langle \tilde{\mathbf{e}}_1, \mathbf{N}_A(\mathbf{v}) \rangle \mathbf{N}_A(\mathbf{v})\|},$$

and

$$\mathbf{e}_2 = \frac{\tilde{\mathbf{e}}_2 - \langle \tilde{\mathbf{e}}_2, \mathbf{N}_A(\mathbf{v}) \rangle \mathbf{N}_A(\mathbf{v}) - \langle \tilde{\mathbf{e}}_2, \mathbf{e}_1 \rangle \mathbf{e}_1}{\|\tilde{\mathbf{e}}_2 - \langle \tilde{\mathbf{e}}_2, \mathbf{N}_A(\mathbf{v}) \rangle \mathbf{N}_A(\mathbf{v}) - \langle \tilde{\mathbf{e}}_2, \mathbf{e}_1 \rangle \mathbf{e}_1\|}.$$

Logically speaking, one can first choose an orthonormal basis $\mathbf{e}_1, \mathbf{e}_2$ for the approximating tangent space $TS_A(v)$ and then apply the Gram-Schmidt process to obtain an orthonormal basis $\tilde{\mathbf{e}}_1, \tilde{\mathbf{e}}_2$ for the tangent plane $T\Sigma(\mathbf{v})$. In either way, we always have by Lemma 2 the following relations.

Lemma 3. *One has*

$$\tilde{\mathbf{e}}_i = \mathbf{e}_i + O(r), \quad i = 1, 2. \quad (27)$$

Consider a neighboring vertex \mathbf{v}_i of \mathbf{v} in V . For r small enough, we can use the inverse of the exponential map $\exp_{\mathbf{p}}$ to lift the vertex \mathbf{v}_i up to the tangent plane $T\Sigma(\mathbf{v})$ and obtain

$$\tilde{\mathbf{v}}_i = \exp_{\mathbf{v}}^{-1}(\mathbf{v}_i) \in T\Sigma(\mathbf{v})$$

and

$$\tilde{\mathbf{v}}_i = \tilde{x}_i \tilde{\mathbf{e}}_1 + \tilde{y}_i \tilde{\mathbf{e}}_2$$

for some constants. As discussed in section 3, we can also lift the vertex \mathbf{v}_i up to the approximating tangent plane $T\Sigma_A(\mathbf{v})$ and get

$$\bar{\mathbf{v}}_i = (\mathbf{v}_i - \mathbf{v}) - \langle \mathbf{v}_i - \mathbf{v}, \mathbf{N}_A(\mathbf{v}) \rangle \mathbf{N}_A(\mathbf{v})$$

and for some constants x_i, y_i . Then Lemmas 2 and 3 yield

Lemma 4. *One has*

$$\begin{cases} \tilde{x}_i = x_i + O(r^2) \\ \tilde{y}_i = y_i + O(r^2). \end{cases} \quad (28)$$

Using these relations, one can solve the configuration equation (15) for $(\tilde{x}_i, \tilde{y}_i)$ and (x_i, y_i) respectively and obtain their corresponding solutions $\tilde{\alpha}_i$ and α_i with the relation

$$\tilde{\alpha}_i = \alpha_i + O(r). \quad (29)$$

Note that the lifting function \tilde{h} is a smooth function of two variables x and y . Equation (17) now gives an approximation of the Laplacian $\Delta \tilde{h}(0, 0)$:

$$\Delta \tilde{h}(0, 0) = \frac{4 \sum_{i=1}^n \tilde{\alpha}_i (\tilde{h}(x_i, y_i) - \tilde{h}(0, 0))}{\sum_{i=1}^n \tilde{\alpha}_i (\tilde{x}_i^2 + \tilde{y}_i^2)} + O(r). \quad (30)$$

The relations (21), (26) and (27) imply

$$\Delta \tilde{h}(0, 0) = \frac{4 \sum_{i=1}^n \alpha_i (h(\mathbf{v}_i) - h(\mathbf{v}))}{\sum_{i=1}^n \alpha_i (x_i^2 + y_i^2)} + O(r). \quad (31)$$

This along with Lemma 1 proves Theorem 1.

For each vertex $\mathbf{v}_i \in V$, we have

$$\Delta_{\Sigma} \phi(\mathbf{v}_i) = \frac{2 \sum_{j=1}^{N(i)} (\alpha_{i,j} (\phi(\mathbf{v}_{i,j}) - \phi(\mathbf{v}_i)))}{\sum_{j=1}^{N(i)} (\alpha_{i,j} x_{i,j}^2)} + O(r). \quad (32)$$

Denote $\omega_i = \frac{2}{\sum_{j=1}^{N(i)} (\alpha_{i,j} x_{i,j}^2)}$. Since $\sum_{j=1}^{N(i)} \alpha_{i,j} = 1$, Equation (32) can be rewritten as

$$\Delta_{\Sigma} \phi(\mathbf{v}_i) = \omega_i \left[\left(\sum_{j=1}^{N(i)} (\alpha_{i,j} \phi(\mathbf{v}_{i,j})) \right) - \phi(\mathbf{v}_i) \right] + O(r). \quad (33)$$

Furthermore the vector $(\alpha_{i,1}, \alpha_{i,2}, \dots, \alpha_{i,N(i)})$ can be easily extended to a $1 \times n_V$ vector $(a_{i,1}, a_{i,2}, \dots, a_{i,n_V})$ by

$$a_{i,k} = \begin{cases} \alpha_{i,j} & \text{if there exists } j \in \{1, 2, \dots, N(i)\} \text{ such that } v_k = v_{i,j}, \\ -1 & \text{if } i = k, \\ 0 & \text{otherwise.} \end{cases} \quad (34)$$

Obviously,

$$\Delta_{\Sigma} \phi(\mathbf{v}_i) = \omega_i [(a_{i,1}, a_{i,2}, \dots, a_{i,n_V})(\phi(\mathbf{v}_1), \phi(\mathbf{v}_2), \dots, \phi(\mathbf{v}_{n_V}))^T] + O(r). \quad (35)$$

Remark 2. $\{1, 2, \dots, n_V\}$ is the set of indices of all vertices in V and \mathbf{v}_i denotes the i th vertex in V . For each $i \in \{1, 2, \dots, n_V\}$, $\{1, 2, \dots, N(i)\}$ is the set of indices of one-neighbors of \mathbf{v}_i and $\mathbf{v}_{i,j}$ denotes the j th one-neighbor of \mathbf{v}_i in $\{\mathbf{v}_{i,1}, \mathbf{v}_{i,2}, \dots, \mathbf{v}_{i,N(i)}\}$. Obviously, every one-neighbor $\mathbf{v}_{i,j}$ of \mathbf{v}_i is corresponding to a unique vertex \mathbf{v}_k in V while j and k may be not equal.

This implies that

$$\begin{pmatrix} \Delta_{\Sigma} \phi(\mathbf{v}_1) \\ \Delta_{\Sigma} \phi(\mathbf{v}_2) \\ \vdots \\ \Delta_{\Sigma} \phi(\mathbf{v}_{n_V}) \end{pmatrix} = WA \begin{pmatrix} \phi(\mathbf{v}_1) \\ \phi(\mathbf{v}_2) \\ \vdots \\ \phi(\mathbf{v}_{n_V}) \end{pmatrix} + O(r), \quad (36)$$

where $W = \text{diag}(\omega_1, \dots, \omega_{n_V})$ and $A = (a_{i,k})$ are two $n_V \times n_V$ matrices. For simplicity, we rewrite Equation (36) as

$$\Delta_{\Sigma} \phi(V) = (WA)\phi(V) + O(r). \quad (37)$$

Hence, we have an eigenvalue approximation result by the method discussed in [18].

Theorem 2. Let Σ be a closed regular surface, $S = (V, F)$ be a triangular mesh of Σ with mesh width r . If λ_i is the i th eigenvalue of the Laplace-Beltrami operator on Σ and $\bar{\lambda}_i$ is the i th eigenvalue of the matrix WA , then we have, for sufficiently small $r > 0$,

$$\lambda_i = \bar{\lambda}_i + O(r).$$

Remark 3. The matrix equation

$$\begin{pmatrix} \Delta_{\Sigma} \phi(\mathbf{v}_1) \\ \Delta_{\Sigma} \phi(\mathbf{v}_2) \\ \vdots \\ \Delta_{\Sigma} \phi(\mathbf{v}_{n_V}) \end{pmatrix} = WA \begin{pmatrix} \phi(\mathbf{v}_1) \\ \phi(\mathbf{v}_2) \\ \vdots \\ \phi(\mathbf{v}_{n_V}) \end{pmatrix} \quad (38)$$

is called the configuration equation of the Laplace-Beltrami operator at \mathbf{v}_i on S . The constants $\alpha_{i,j}$ are called the configuration coefficients of Laplace-Beltrami operator at \mathbf{v}_i on S . The $n_V \times n_V$ matrix A defined in Equation (34) is called the configuration matrix of the Laplace-Beltrami operator on S .

3.2. The Configuration matrix for $\nabla_\Sigma \cdot (h\nabla_\Sigma\phi)$

Let h be a bounded smooth function defined on a regular surface Σ . We introduce the configuration matrix of the quantity $\nabla_\Sigma \cdot (h\nabla_\Sigma\phi)$ by a similar method as in subsection 3.1. First, let us consider two smooth functions f and g defined on an open domain Ω in \mathbb{R}^2 with the original point $(0,0) \in \Omega$. Since $\nabla_\Sigma \cdot (h\nabla_\Sigma\phi) = \nabla_\Sigma h \cdot \nabla_\Sigma\phi + h\Delta_\Sigma\phi$, we need to estimate the quantity $\nabla g \cdot \nabla f + g\Delta f = g_x f_x + g_y f_y + g(f_{xx} + f_{yy})$ in \mathbb{R}^2 . Taylor expansions of f and g are given by

$$\begin{aligned} f(x, y) - f(0, 0) &= x f_x(0, 0) + y f_y(0, 0) \\ &\quad + \frac{x^2}{2} f_{xx}(0, 0) + xy f_{xy}(0, 0) \\ &\quad + \frac{y^2}{2} f_{yy}(0, 0) + O(r^3) \end{aligned} \quad (39)$$

and

$$\begin{cases} f(x, y) - f(0, 0) = x f_x(0, 0) + y f_y(0, 0) + O(r^2) \\ g(x, y) - g(0, 0) = x g_x(0, 0) + y g_y(0, 0) + O(r^2), \end{cases} \quad (40)$$

when $r = x^2 + y^2$ is small. From Equation (40), one has

$$\begin{aligned} &(f(x, y) - f(0, 0))(g(x, y) - g(0, 0)) \\ &= (x f_x(0, 0) + y f_y(0, 0))(x g_x(0, 0) + y g_y(0, 0)) + O(r^3) \\ &= x^2 f_x(0, 0) g_x(0, 0) + xy (f_x(0, 0) g_y(0, 0) + f_y(0, 0) g_x(0, 0)) \\ &\quad + y^2 f_y(0, 0) g_y(0, 0) + O(r^3). \end{aligned} \quad (41)$$

These imply

$$\begin{aligned} &(f(x, y) - f(0, 0))(g(x, y) - g(0, 0)) + 2g(0, 0)(f(x, y) - f(0, 0)) \\ &= 2xg(0, 0)f_x(0, 0) + 2yg(0, 0)f_y(0, 0) + xy(2g(0, 0)f_{xy}(0, 0) + f_x(0, 0)g_y(0, 0) \\ &\quad + f_y(0, 0)g_x(0, 0)) + x^2(g(0, 0)f_{xx}(0, 0) + f_x(0, 0)g_x(0, 0)) \\ &\quad + y^2(g(0, 0)f_{yy}(0, 0) + f_y(0, 0)g_y(0, 0)) + O(r^3). \end{aligned} \quad (42)$$

Consider a family of neighboring points $(x_j, y_j) \in \Omega$, $j = 1, 2, \dots, n$, of the origin $(0, 0)$. Take some constants $\beta_j, j = 1, 2, \dots, n$ with $\sum_{j=1}^n \beta_j = 1$. We

have

$$\begin{aligned}
& \sum_{j=1}^n [(f(x_j, y_j) - f(0, 0)) (g(x_j, y_j) - g(0, 0)) + 2g(0, 0)(f(x_j, y_j) - f(0, 0))] \\
&= \left(\sum_{j=1}^n \beta_j x_j \right) 2g(0, 0) f_x(0, 0) + \left(\sum_{j=1}^n \beta_j y_j \right) 2g(0, 0) f_y(0, 0) \\
&\quad + \left(\sum_{j=1}^n \beta_j x_j y_j \right) (2g(0, 0) f_{xy}(0, 0) + f_x(0, 0) g_y(0, 0) + f_y(0, 0) g_x(0, 0)) \\
&\quad + \left(\sum_{j=1}^n \beta_j x_j^2 \right) (g(0, 0) f_{xx}(0, 0) + f_x(0, 0) g_x(0, 0)) \\
&\quad + \left(\sum_{j=1}^n \beta_j y_j^2 \right) (g(0, 0) f_{yy}(0, 0) + f_y(0, 0) g_y(0, 0)) + O(r^3).
\end{aligned} \tag{43}$$

To compute $\nabla g \cdot \nabla f + g \Delta f$ at $(0, 0)$, we choose the constants β_j , $j = 1, 2, \dots, n$, so that they satisfy the following equations:

$$\begin{pmatrix} x_1, & x_2, & \dots, & x_n \\ y_1, & y_2, & \dots, & y_n \\ x_1 y_1, & x_2 y_2, & \dots, & x_n y_n \\ x_1^2 - y_1^2, & x_2^2 - y_2^2, & \dots, & x_n^2 - y_n^2 \\ 1, & 1, & \dots, & 1 \end{pmatrix} \begin{pmatrix} \beta_1 \\ \beta_2 \\ \vdots \\ \beta_n \end{pmatrix} = \begin{pmatrix} 0 \\ 0 \\ 0 \\ 0 \\ 1 \end{pmatrix}, \tag{44}$$

The solutions β_j of this equation gives a formula for $\nabla g \cdot \nabla f + g \Delta f$ at $(0, 0)$:

$$\begin{aligned}
& (\nabla g \cdot \nabla f + g \Delta f)(0, 0) \\
&= g_x(0, 0) f_x(0, 0) + g_y(0, 0) f_y(0, 0) + g(0, 0) [f_{xx}(0, 0) + f_{yy}(0, 0)] \\
&= \frac{1}{\sum_{j=1}^n \beta_j x_j^2} \sum_{j=1}^n [(f(x_j, y_j) - f(0, 0)) (g(x_j, y_j) - g(0, 0)) \\
&\quad + 2g(0, 0)(f(x_j, y_j) - f(0, 0))] + O(r) \\
&= \frac{\sum_{j=1}^n (f(x_j, y_j) - f(0, 0))(g(x_j, y_j) - g(0, 0))}{\sum_{j=1}^n \beta_j x_j^2} + O(r)
\end{aligned} \tag{45}$$

Using the notations of subsection 3.1, the quantity $\Delta_S(h\Delta_S\phi)$ at \mathbf{v}_i on S is

given by

$$\nabla_S(h\nabla_S\phi)(\mathbf{v}_i) = \frac{\sum_{j=1}^{N(i)} (\beta_{i,j}(f(x_i, y_i) - f(0, 0))(g(x_i, y_i) + g(0, 0)))}{\sum_{j=1}^{N(i)} \beta_{i,j}x_{i,j}^2}. \quad (46)$$

Then one can prove

Theorem 3. *Given two smooth functions h, ϕ on a closed regular surface Σ with a triangular surface mesh $S = (V, F)$, one has*

$$\nabla_\Sigma(h\nabla_\Sigma)(\mathbf{v}_i) = \nabla_S(h\nabla_S\phi)(\mathbf{v}_i) + O(r) \quad (47)$$

where the quantity $\nabla_S(h\nabla_S\phi)(\mathbf{v}_i)$ is given in Equation (46) and r is the mesh size of S .

Remark 4. *The error terms $O(r)$ in Theorems 1, 2 and 3 depend only on some geometric invariants of S and the function f since Σ is a closed regular surface.*

Similarly, We extend these scalars $\beta_{i,j}$ for each $i \in \{1, 2, \dots, n_V\}$ and for each $j \in \{1, 2, \dots, N(i)\}$ to a $n_V \times n_V$ matrix $B = (b_{i,k})$ with

$$b_{i,k} = \begin{cases} \beta_{i,j} & \text{if there exists } j \in \{1, 2, \dots, N(i)\} \text{ such that } v_k = v_{i,j}, \\ -1 & \text{if } i = k, \\ 0 & \text{otherwise.} \end{cases} \quad (48)$$

And, we have

$$\begin{pmatrix} \nabla_\Sigma(h\nabla_\Sigma\phi)(\mathbf{v}_1) \\ \nabla_\Sigma(h\nabla_\Sigma\phi)(\mathbf{v}_2) \\ \vdots \\ \nabla_\Sigma(h\nabla_\Sigma\phi)(\mathbf{v}_{n_V}) \end{pmatrix} = WB \begin{pmatrix} \phi(\mathbf{v}_1) \\ \phi(\mathbf{v}_2) \\ \vdots \\ \phi(\mathbf{v}_{n_V}) \end{pmatrix} + O(r), \quad (49)$$

where $W = \text{diag}(\omega_1, \dots, \omega_{n_V})$, $\omega_i = \frac{1}{\sum_{j=1}^{N(i)} \alpha_{i,j}x_{i,j}^2}$.

4. High-order approximations

In this section we shall discuss how to use the LTL method to obtain high-order approximations of these differential operators. The ideas are very simple. First, we shall propose an algorithm to construct a high-order approximation of the underlying surface. Second, we also give a method to obtain a high-order approximation of smooth functions on. Third, using these approximations, we can compute the differential quantities under consideration with high-order accuracies.

As before, we consider a triangular surface mesh $S = (V, F)$, of the smooth surface Σ where $V = \{\mathbf{v}_i | 1 \leq i \leq n_V\}$ with mesh size $r > 0$ is the list of

vertices and $F = \{T_k | 1 \leq k \leq n_F\}$ is the list of triangles. To obtain a high-order approximation of the underlying surface Σ around a vertex \mathbf{v} , we will try to construct a local parametrization by representing the smooth surface Σ as locally a graph surface around the vertex \mathbf{v} . Let $N_A(\mathbf{v})$ be the approximating normal vector at the vertex \mathbf{v} in S as \mathbf{v} in (8). The approximating tangent plane $TS_A(\mathbf{v})$ of S at \mathbf{v} is given by $TS_A(\mathbf{v}) = \{\mathbf{w} \in \mathbb{R}^3 | \mathbf{w} \perp N_A(\mathbf{v})\}$.

We can choose an orthonormal basis $\mathbf{e}_1, \mathbf{e}_2$ for the approximating tangent plane $TS_A(\mathbf{v})$ of S at \mathbf{v} and obtain an orthonormal coordinates (x, y) for vectors $\mathbf{w} \in TS_A(\mathbf{v})$ by $\mathbf{w} = x\mathbf{e}_1 + y\mathbf{e}_2$. The approximating tangent plane is nearly tangential to the surface and the z -coordinate is orthogonal to the xy -plane, the approximating tangent plane $TS_A(\mathbf{v})$, and corresponds to the height function h . That is, for every point p in Σ around \mathbf{v} we can assign it an xyz -coordinates as follows:

$$(\mathbf{p} - \mathbf{v}) - \langle \mathbf{p} - \mathbf{v}, N_A(\mathbf{v}) \rangle N_A(\mathbf{v}) = x(\mathbf{p})\mathbf{e}_1 + y(\mathbf{p})\mathbf{e}_2 \quad (50)$$

and

$$h(x(\mathbf{p}), y(\mathbf{p})) = \langle \mathbf{p} - \mathbf{v}, N_A(\mathbf{v}) \rangle \quad (51)$$

The n -ring ($n > 1$) neighboring vertex \mathbf{v}_i of \mathbf{v} in V is now given as

$$x_i = x(\mathbf{v}_i), \quad y_i = y(\mathbf{v}_i), \quad z_i = h(x_i, y_i) \quad (52)$$

in the xyz -space. To give locally a high-order surface reconstruction of Σ , we only need to find a suitable polynomial fitting for the height function h with high-order accuracy by using the local data $z_i = h(x_i, y_i)$. This can be done by employing the high-order Taylor expansion again as we did in the previous section.

The height function h can be approximating to k th-order accuracy about the origin $\mathbf{o} = (0, 0)$ as

$$h(x, y) = \sum_{d=0}^k \sum_{m=0}^d c_{d,m} \frac{x^{d-m} y^m}{(d-m)!m!} + O(r^{d+1}) \quad (53)$$

where the constant $c_{d,m} = \frac{\partial^d}{\partial x^{d-m} \partial y^m} h(0, 0)$. In particular, one has $c_{0,0} = h(0, 0)$. Since the regular surface Σ is smooth, the height function h is locally smooth and has $k+1$ continuous derivatives. We assume that the $\frac{j}{2}$ -ring ($j \geq 2$) neighboring vertices \mathbf{v}_i of \mathbf{v} in V is near the vertex \mathbf{v} . Since these vertices \mathbf{v}_i sample the surface Σ near the vertex \mathbf{v} , their coordinates in the xyz -space allow us to obtain the equation:

$$h(x_i, y_i) - h(0, 0) = \sum_{d=0}^k \sum_{m=0}^d e_{d,m} \frac{x_i^{d-m} y_i^m}{(d-m)!m!} \quad (54)$$

Let $n = \frac{(k+1)(k+2)}{2} - 1$ be the total number of coefficients $e_{d,m}$. We can choose n nearest neighboring vertices \mathbf{v}_i of \mathbf{v} to solve the equation (54) by the configuration method in section 3 and obtain a set of solution for the coefficients $e_{d,m}$. That is, we can find constants $\alpha_{s,t}^i$ $i = 1, 2, \dots, n$ with $(s, t) \neq (0, 0)$ so that

$$\sum_{i=1}^n \alpha_{s,t}^i \frac{x_i^{d-m} y_i^m}{(d-m)!m!} = \begin{cases} 1 & \text{when } (d, m) = (s, t) \\ 0 & \text{when } (d, m) \neq (s, t) \end{cases} \quad (55)$$

Hence we have

$$e_{s,t} = \sum_{i=1}^n \alpha_{s,t}^i [h(x_i, y_i) - h(0, 0)] \quad (56)$$

Moreover, we have the following approximation:

$$c_{d,m} = e_{d,m} + O(r^{k+1-d}). \quad (57)$$

Next we discuss how to approximate a smooth function ϕ with high-order accuracy. Consider a smooth function ϕ on Σ . We can view ϕ as a function of x and y near the vertex \mathbf{v} . That is, we have locally, for a point \mathbf{p} near \mathbf{v} with local coordinates $(x, y, h(x, y))$,

$$\phi(x, y) = \phi(\mathbf{p}) \quad (58)$$

Again we can use the local data $\phi(x_i, y_i) = \phi(\mathbf{p})$ to approximate the function ϕ with k th-order accuracy about the origin $\mathbf{o} = (0, 0)$ by applying the configuration method to the k th-order Taylor expansion of the function ϕ as we just discussed above for the height function h .

Once we have the local high-order polynomial approximations of the height function around the vertex $\mathbf{v} \in \Sigma$ and the smooth function ϕ on Σ , we can also get high-order approximation of the normal vectors, curvatures at the vertex \mathbf{v} and the gradient, Laplacian of ϕ .

As we just discussed above, the regular surface Σ is locally a graph surface around the vertex $\mathbf{v} \in \Sigma$. That is, we can find locally a smooth height function of two variables $z = h(x, y)$, $(x, y) \in \Omega \subset \mathbb{R}^2$ so that locally we have the associated graph surface $\Sigma = \{(x, y, h(x, y)) | (x, y) \in \Omega\}$ around the vertex \mathbf{v} . The local graph surface Σ has a natural parametrization:

$$\mathbf{X}(u, v) = (u, v, h(u, v)), \quad (u, v) \in \Omega. \quad (59)$$

Hence, we have the tangent vectors

$$\mathbf{X}_u = (1, 0, h_u) \text{ and } \mathbf{X}_v = (0, 1, h_v) \quad (60)$$

and their derivative

$$\mathbf{X}_{uu} = (0, 0, h_{uu}), \quad \mathbf{X}_{uv} = (0, 0, h_{uv}) \text{ and } \mathbf{X}_{vv} = (0, 0, h_{vv}) \quad (61)$$

This gives the unit normal vector

$$\mathbf{N}(u, v) = \frac{(-h_u, -h_v, 1)}{\sqrt{h_u^2 + h_v^2 + 1}}, \quad (u, v) \in \Omega. \quad (62)$$

The coefficients of the first fundamental form E, F, G of the graph surface Σ are given by

$$E = 1 + h_u^2, \quad F = h_u h_v, \quad G = 1 + h_v^2 \quad (63)$$

and hence we have $EG - F^2 = 1 + h_u^2 + h_v^2$. And, the coefficients e, f, g of the second fundamental form of Σ are given by

$$e = \frac{h_{uu}}{\sqrt{1 + h_u^2 + h_v^2}}, \quad f = \frac{h_{uv}}{\sqrt{1 + h_u^2 + h_v^2}} \quad \text{and} \quad g = \frac{h_{vv}}{\sqrt{1 + h_u^2 + h_v^2}}. \quad (64)$$

The formulas for Gaussian and mean curvatures are given by

$$K = \frac{h_{uu}h_{vv} - h_{uv}^2}{(1 + h_u^2 + h_v^2)^2} \quad \text{and} \quad H = \frac{1}{2} \frac{(1 + h_u^2)h_{vv} - 2h_u h_v h_{uv} + (1 + h_v^2)h_{uu}}{(1 + h_u^2 + h_v^2)^{3/2}} \quad (65)$$

Consider a smooth function ϕ on the graph surface Σ . The gradient $\nabla_\Sigma \phi$ of ϕ can be computed from equation (5) and one yields

$$\nabla_\Sigma \phi = \frac{(\phi_u(1 + h_u^2) - \phi_v h_u h_v, \phi_v(1 + h_v^2) - \phi_u h_u h_v, \phi_u + \phi_v)}{1 + h_u^2 + h_v^2} \quad (66)$$

where $\phi_u = \frac{\partial \phi(\mathbf{X}(u, v))}{\partial u}$ and $\phi_v = \frac{\partial \phi(\mathbf{X}(u, v))}{\partial v}$. Similarly, we can use Equations (5)-(7) to compute the divergence of a vector field \mathbf{V} and the Laplacian $\Delta_\Sigma \phi$ of a smooth function ϕ on the graph surface Σ .

From these equations, we can conclude that if we have k th-order polynomial approximations of the height function h around the vertex $\mathbf{v} \in \Sigma$ and the smooth function ϕ on Σ , we obtain $(k-1)$ th-order approximations for the normal vector, E, F, G and the gradient of ϕ . We also obtain $(k-2)$ th-order approximations for the Gaussian and mean curvatures and also the Laplacian of ϕ on Σ .

5. Numerical simulations

In this section, we present some numerical simulations of our proposed methods in sections 3 and 4. The models in our simulations are the unit sphere, the torus with inner radius 0.5 and outer radius 1, a dumbbell with the parametrization

$$\mathbf{X}(u, v) = (r \sin v \cos u, \quad r \sin v \sin u, \quad r \cos v) \quad (67)$$

where $r = \sqrt{0.9^2 \cos(2x) + \sqrt{1 - 0.9^4 \sin^2(2x)}}$, see Figure 2, and a wave surface with

$$\mathbf{X}(u, v) = (u, v, \sin u \cos(v)), \quad (68)$$

where $(u, v) \in [0, 2\pi] \times [0, 2\pi]$, see Figure 3.

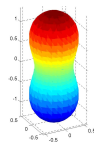


Figure 2: The figure of a dumbbell

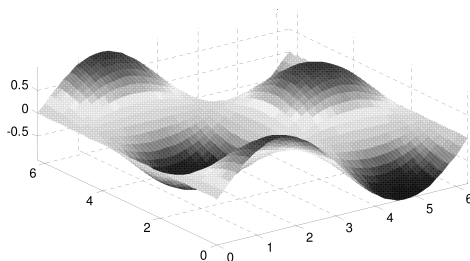


Figure 3: The figure of the wave surface

5.1. Simulations for the $O(r)$ -LTL algorithm

First, we show the numerical solutions of eigenvalues of Laplace-Beltrami operator on the unit sphere and some curved surfaces by the $O(r)$ -LTL method in section 3.1. The $O(r)$ -LTL approach is a special case for our $O(r^n)$ -LTL method. Although the $O(r)$ -LTL method has a lower convergent rate, it only requires at least 5 neighboring vertices of each vertex on the surfaces and the triangular meshes always can be reconstructed such that the number of 1-ring neighboring vertices of each vertex is at least 5.

Table 1 shows the simulation results of the eigenvalues and its multiplicity of the Laplace-Beltrami operator on the unit sphere by our $O(r)$ -LTL method. The triangular mesh sizes of the unit sphere in our simulations are 0.32, 0.16, 0.08 and 0.04. We give these triangular meshes in Figure 4. Figure 7 gives some eigenfunctions on the torus with inner radius 0.5 and outer radius 1 and Figure 6 shows all eigenfunctions corresponding to the first 5 eigenvalues on a unit sphere by the $O(r)$ -LTL method.

Figure 5 shows the convergence result of the eigenvalues of a unit hemisphere by our $O(r)$ -LTL method. Our $O(r)$ -LTL method has the quadratic convergence.

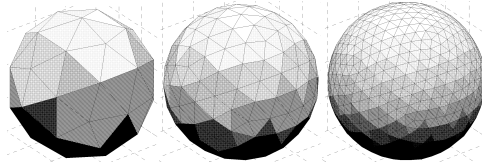


Figure 4: The subdivision of triangular meshes of a unit sphere by $O(r)$ -LTL method

Table 1: The eigenvalues and its multiplicity of a unit sphere

mesh size	1st eigenvalue (multiplicity)	2nd eigenvalue (multiplicity)	3th eigenvalue (multiplicity)
0.32	-2.0484 (3)	-6.0014 (5)	-11.5986 (7)
0.16	-2.0117 (3)	-6.0002 (5)	-11.8998 (7)
0.08	-2.0029 (3)	-6.0 (5)	-11.9735 (7)
0.04	-2.0 (3)	-6.0 (5)	-12.0 (7)

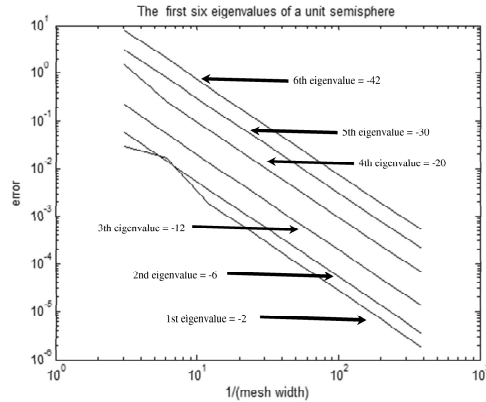


Figure 5: The left shows some eigenfunctions of a hemisphere by $O(r)$ -LTL method. The right is a convergence study for the first six eigenvalues of a unit hemisphere.

5.2. Simulations for the $O(r^n)$ -LTL algorithm with $n \geq 2$

In this subsection, we compute the Laplacian of a function,

$$F(u, v) = \exp(0.5 \sin u + \cos^3 v) \quad (69)$$

where (u, v) defined on the domain of $\mathbf{X}(u, v)$ in Equation (68), on the parametric surface in Equation (68) by high-order algorithms. How to determine the necessary neighboring vertices of a given vertex is an important problem for high-order accuracies. Ray et al.[15] proposed an elegant method to improve this problem by using the $\frac{j}{2}$ -ring ($j \geq 2$) for neighboring vertices, see Figure 8. We will also use the $\frac{j}{2}$ -ring neighboring vertices in our simulations.

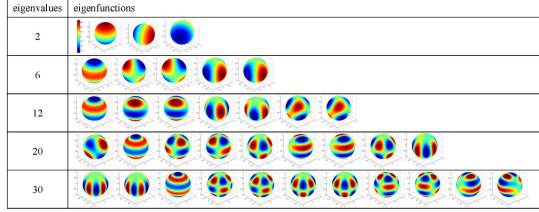


Figure 6: The eigenfunctions of the Laplace-Beltrami operator on a unit sphere by $O(r)$ -LTL method.

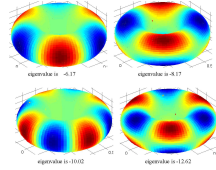


Figure 7: The eigenfunctions of the Laplace-Beltrami operator on a torus by $O(r)$ -LTL method.

We estimate the l^∞ relative error of Laplacian on each mesh as

$$l^\infty \text{ relative error} = \max_{\mathbf{v}_i \in V} (\text{relative error at } \mathbf{v}_i) \quad (70)$$

where

$$\text{relative error at } \mathbf{v}_i = \frac{\| \text{numerical solution at } \mathbf{v}_i - \text{reference solution at } \mathbf{v}_i \|}{\| \text{reference solution at } \mathbf{v}_i \|} \quad (71)$$

and $\| \text{reference solution at } \mathbf{v}_i \| \neq 0$.

Figure 9 shows the l^∞ relative errors of Laplacian of the function $F(u, v) = \exp(0.5 \sin u + \cos^3 v)$ in the interior vertices on this parametric surface. These results always converge to the exact Laplacian when the mesh size of the triangular mesh approaches 0.

Now, we compare the eigenvalues and eigenfunctions on a unit sphere. It is well-known that the n -th nonzero eigenvalues of the Laplace-Beltrami operator

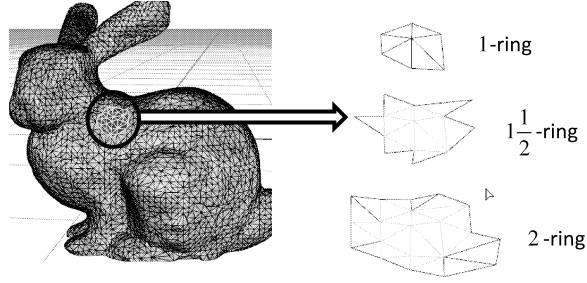


Figure 8: The 1, $1\frac{1}{2}$ and 2-rings of a vertex on the bunny model.

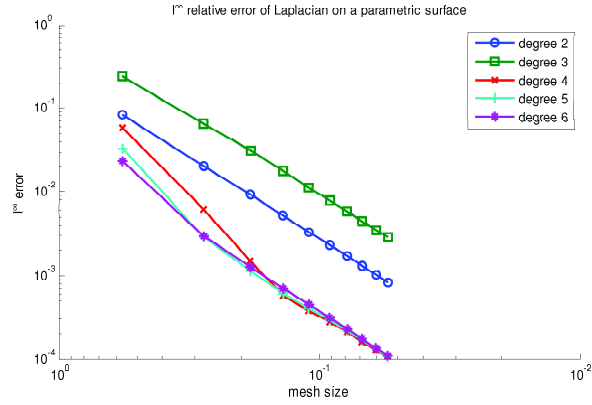


Figure 9: The l^∞ relative errors of laplacian of the function $F(u, v) = \exp(0.5 \sin u + \cos^2 v)$ in Equation on a wave surface in Equation (68)

on the unit sphere are $-n(n+1)$ with multiplicity $(2n+1)$. The eigenfunctions of the unit sphere are restrictions on the unit sphere of harmonic homogeneous polynomials in \mathbb{R}^3 . Figures 10 and 11 show the errors of the eigenvalues $\lambda = 2$ and 6 on a unit sphere, respectively. For the error $e(h_1)$ and $e(h_2)$ for the mesh size h_1 and h_2 the experimental error of convergence is defined as

$$EOC(h_1, h_2) = \log \frac{e(h_1)}{e(h_2)} \left(\log \frac{h_1}{h_2} \right)^{-1}. \quad (72)$$

Tables 2 and 3 show the EOC of the first and second eigenvalues on the unit sphere, respectively.

Let $\{\phi_{n,i}\}_{i=1}^{2n+1}$ be the set of eigenfunctions corresponding to the eigenvalue $-n(n+1)$ on the unit sphere and let $\tilde{\phi}_{n,i}$ be the approximated solution by our $O(r^n)$ -LTL method. Then we choose $\bar{\phi}_{n,i}$ to be the linear combination $\sum_{i=1}^{2n+1} \alpha_i \phi_{n,i}$ so that it realizes the minimum of $\|\sum_{i=1}^{2n+1} \beta_j \phi_{n,i} - \tilde{\phi}_{n,i}\|$ over β_j 's. The error E_n of the nth eigenvalue with eigenfunctions $\bar{\phi}_{n,i}$ and the ap-

Table 2: EOC of the 1st eigenvalue on a unit sphere

mesh size	degree 2	degree 3	degree 4	degree 5	degree 6
0.5443	-	-	-	-	-
0.2774	2.0971	1.9543	3.6868	4.1610	6.7939
0.1877	2.0901	1.9751	4.1204	3.8777	5.9443
0.1407	2.0049	1.9327	4.0126	3.8251	6.1007
0.1130	2.0384	1.9872	4.0847	3.9515	6.2562
0.0941	1.9998	1.9626	4.0049	3.9122	5.9561
0.0807	2.0243	1.9949	4.0537	3.9847	6.9588
0.0706	1.9989	1.9754	3.9973	3.9468	5.8779

Table 3: EOC of the 2nd eigenvalue on a unit sphere

mesh size	degree 2	degree 3	degree 4	degree 5	degree 6
0.5443	-	-	-	-	-
0.2774	1.8991	3.4314	2.8961	5.3251	5.9809
0.1877	2.0115	4.0060	3.7518	5.8448	5.2146
0.1407	1.9552	3.9231	3.7957	5.3624	3.8108
0.1130	1.9999	4.0148	3.9412	5.2539	3.8859
0.0941	1.9691	3.9537	3.9086	4.9920	3.7684
0.0807	1.9981	4.0113	3.9810	4.8949	3.7388
0.0706	1.9765	3.9473	3.9413	5.1215	3.6412

proximating eigenfunctions $\tilde{\phi}_{n,i}$ is defined by

$$E_n = \sup_{i \in \{1, 2, \dots, 2n+1\}} (\|\bar{\phi}_{n,i} - \tilde{\phi}_{n,i}\|_{l^\infty}). \quad (73)$$

Figures 12 and 13 show the errors E_n in Equation (73) of the 1st and 2nd eigenvalues on a unit sphere, respectively.

5.3. Geometric invariants on curved surface

Finally, we estimate the normal vectors and the tensor of curvatures on regular surfaces. Figures 14 - 16 show the l^∞ relative errors of normal vectors, Gaussian curvatures and mean curvatures on a torus with the inner radius 0.5 and the outer radius 1. Figures 17 - 18 give the l^∞ relative errors of normal vectors, Gaussian curvatures and mean curvatures on a dumbbell in Equation (67) and Figure 19 shows the l^∞ errors of Gaussian curvatures on a wave surface. Obviously, the high-order algorithm is much more accurate than the low-order algorithm when the mesh size is small enough.

6. Dissusions and Conclusions

In 2012, Ray et al. also proposed a high-order numerical method for estimating the derivatives and integrations over discrete surfaces. Ray et al. solved the

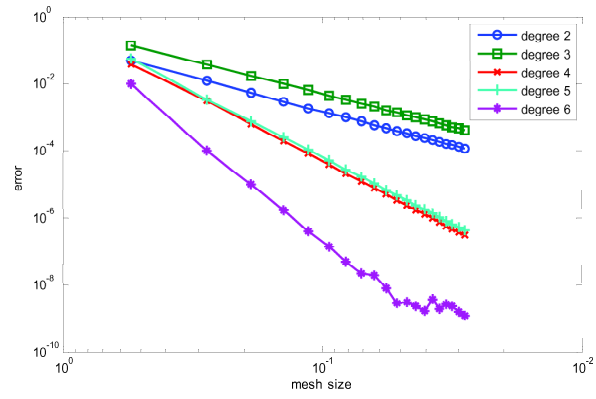


Figure 10: The errors of the 1st eigenvalues on a unit sphere.

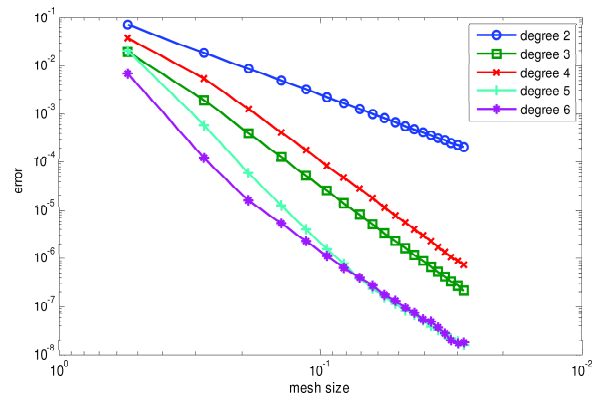


Figure 11: The l^∞ errors of the 2nd eigenvalues on a unit sphere.

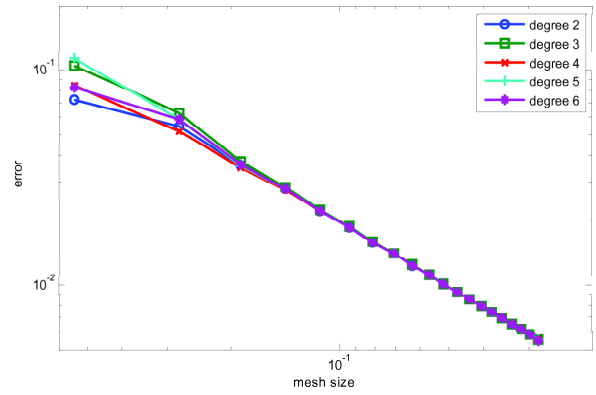


Figure 12: E_1 on a unit sphere.

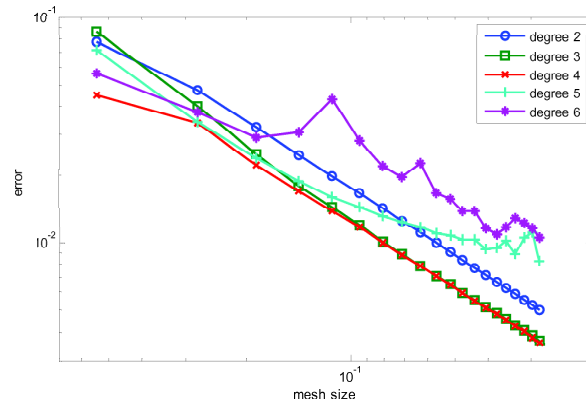


Figure 13: E_2 on a unit sphere.

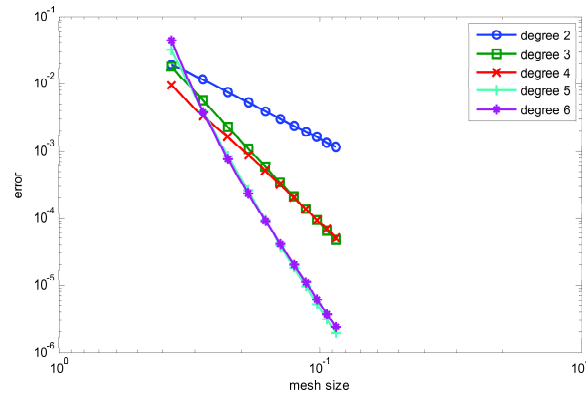


Figure 14: The l^∞ relative errors of normal vectors on a torus

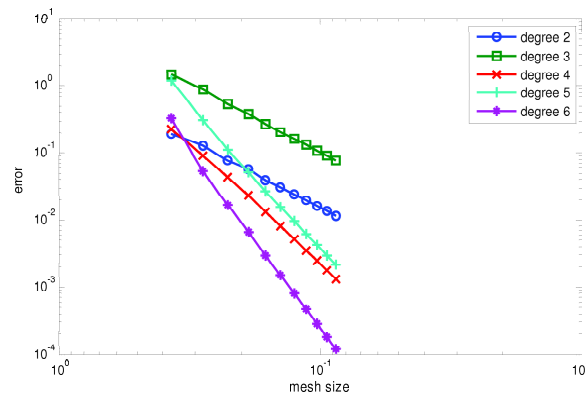


Figure 15: The l^∞ relative error of Gaussian curvatures on a torus

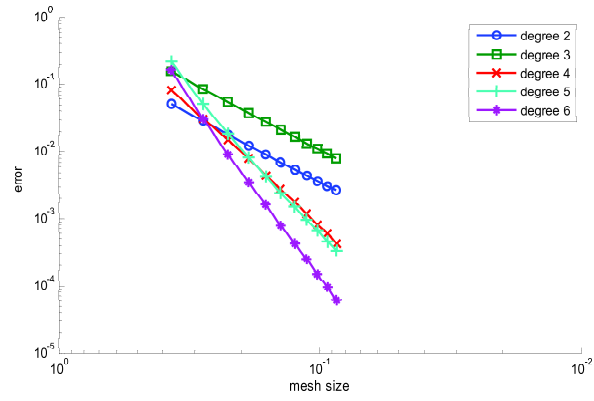


Figure 16: The l^∞ relative error of mean curvatures on a torus

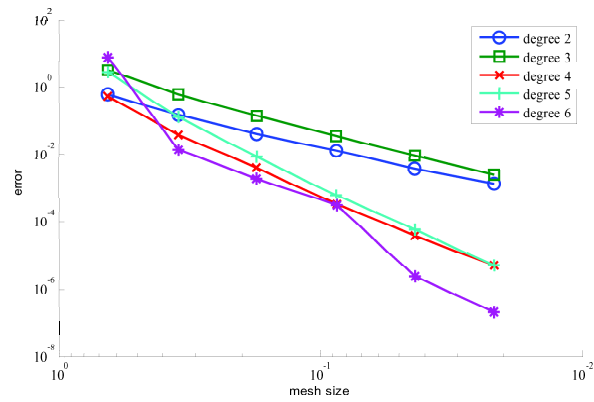


Figure 17: The l^∞ relative errors of Gaussian curvatures on a dumbbell

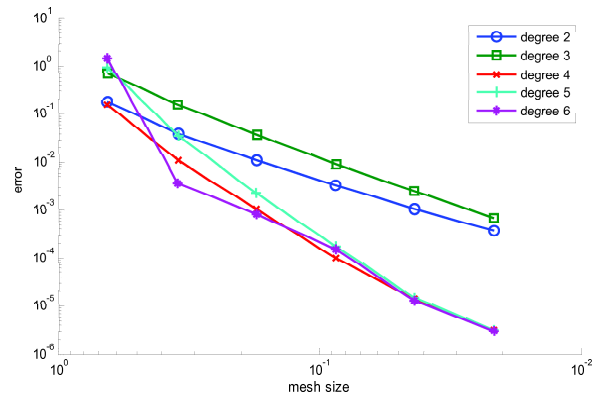


Figure 18: The l^∞ relative error of mean curvatures on a dumbbell

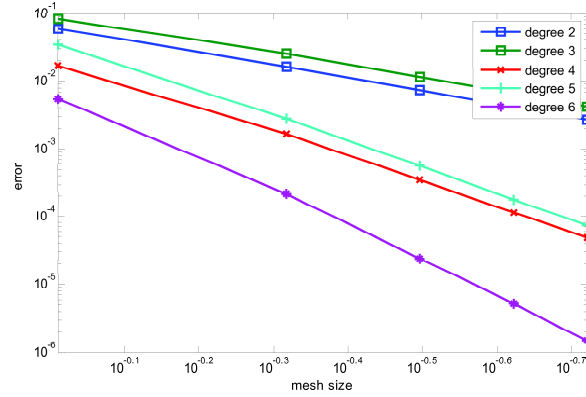


Figure 19: The l^∞ relative error of Gaussian curvatures on a wave surface

system of linear equations from Taylor expansion by the least square method. However, we deal with these problems from the viewpoint of duality and obtain our configuration equations for the Laplace-Beltrami operators over discrete surfaces. The configuration equation for Laplace-Beltrami operator is

$$\begin{pmatrix} x_1, & x_2, & \cdots, & x_n \\ y_1, & y_2, & \cdots, & y_n \\ \frac{x_1^2}{2}, & \frac{x_2^2}{2}, & \cdots, & \frac{x_n^2}{2} \\ x_1y_1 & x_2y_2, & \cdots, & x_ny_n \\ \frac{y_1^2}{2}, & \frac{y_2^2}{2}, & \cdots, & \frac{y_n^2}{2} \end{pmatrix} \begin{pmatrix} \alpha_1 \\ \alpha_2 \\ \vdots \\ \alpha_n \end{pmatrix} = \begin{pmatrix} 0 \\ 0 \\ 1 \\ 0 \\ 1 \end{pmatrix} \quad (74)$$

and the Laplacian $\Delta f(0, 0)$ in Equation (16) is given by

$$\Delta f(0, 0) = \sum_{i=1}^n \alpha_i (f(x_i, y_i) - f(0, 0)). \quad (75)$$

Similarly, we can also obtain a high-order configuration equation for the Laplace-Beltrami operator in the $O(r^n)$ -LTL method.

Although the solution of the configuration equation may not be unique in general, the convergence rates of all solutions are similar by the theoretical analysis. However, not every solution has a good numerical simulation. Finding a suitable solution $\{\alpha_i\}_{i=1}^n$ is a key problem in Ray's method and our $O(r^n)$ -LTL methods. In Ray's method, this problem can be improved by using the conditional number[15]. The pseudo inverse of the configuration matrix is a good approach to handle this problem in our $O(r^n)$ -LTL methods. Hence, we have

$$\begin{pmatrix} \alpha_1 \\ \alpha_2 \\ \vdots \\ \alpha_n \end{pmatrix} = \text{pinv} \left(\begin{pmatrix} x_1, & x_2, & \cdots, & x_n \\ y_1, & y_2, & \cdots, & y_n \\ x_1y_1, & x_2y_2, & \cdots, & x_ny_n \\ x_1^2 - y_1^2, & x_2^2 - y_2^2, & \cdots, & x_n^2 - y_n^2 \\ 1, & 1, & \cdots, & 1 \end{pmatrix} \right) \begin{pmatrix} 0 \\ 0 \\ 0 \\ 0 \\ \epsilon \end{pmatrix} \quad (76)$$

in Equation (15) where $\text{pinv}(\mathbf{M})$ is the pseudo inverse of the matrix \mathbf{M} .

As expected, the high-order approach is more accurate than the low-order approach. However, the low-order approach is more stable than the high-order approach in our simulations. When we use the high-order approach, we need more neighboring vertices at each vertex and the structure of $\frac{1}{2}$ -ring becomes more complicated. For instance we need at least 26 neighboring vertices for the degree 6 approximations.

Note that our $O(r)$ -LTL method is a special case of the $O(r^n)$ -LTL methods. In the $O(r)$ -LTL method, we only need 5 neighboring vertices at each vertex for estimating the Laplacian of a function on a surface by the configuration equation (15). Almost all vertices on a closed triangular mesh can be reconstructed so that the number of 1-ring is at least 5 for each vertex in the new mesh. Ray's method and our high-order configuration equation, Equation (74), need at least 6 neighboring vertices. Indeed, our $O(r)$ -LTL method for estimating Laplacian is a generalization of the well-known the 5- point Laplacian method in \mathbb{R}^2 .

In our $O(r)$ -LTL configuration method, Equations (1) and (2) can be reduced to the matrix equations

$$(WA)(\phi(V)) = \lambda(\phi(V))$$

and

$$(WB)(\phi(V)) = \lambda(\phi(V)),$$

respectively. The configuration masks $A = (a_{i,k}), B = (b_{i,k})$ are given by

$$a_{i,k} = \begin{cases} \alpha_{i,j} & \text{if } v_k = v_{i,j}, \\ -1 & \text{if } i = k, \\ 0 & \text{otherwise,} \end{cases} \quad (77)$$

and

$$b_{i,k} = \begin{cases} \beta_{i,j} & \text{if } v_k = v_{i,j}, \\ -1 & \text{if } i = k, \\ 0 & \text{otherwise,} \end{cases} \quad (78)$$

where $\alpha_{i,j}$ is a solution of Equation (15) and $\beta_{i,j}$ is a solution of Equation (44). Using the configuration matrix A , we can also solve the diffusion equation

$$u_t - \Delta_{\Sigma}u = f$$

on regular surface Σ easily. Furthermore, our $O(r^n)$ -LTL configuration method can also solve general partial differential equations, $L(u) = f$, on a regular surface Σ or on more complicated domains, like Koch snowflakes. The key of our $O(r^n)$ -LTL configuration method for solving the PDE $L(u) = f$ is to find the configuration matrix of the differential operator L on the surface Σ .

It is worth to point out that our $O(r^n)$ -LTL configuration method is effective to solve the eigenpair problems with high-order accuracies even when the underlying surfaces or domains have complicated topological or geometrical structures.

In the near future, we shall extend our $O(r^n)$ -LTL configuration method to solve more partial differential equations on regular surfaces.

Acknowledgment

This paper is partially supported by NSC, Taiwan.

References

- [1] S.-G. Chen, J.-Y. Wu, Estimating normal vectors and curvatures by centroid weights, *Computer Aided Geometric Design* 21 (2004) 447-458.
- [2] S.-G. Chen, J.-Y. Wu, A geometric interpretation of weighted normal vectors and application, *Proceeding of the IEEE Computer Society Conference on Computer Graphics, Imaging and Visualization, New Trends* (2005) 422-425.
- [3] S.-G. Chen, M.-H. Chi, J.-Y. Wu, Curvature estimation and curvature flow for digital curves, *WSEAS transactions on computers* 5 (2006)804-809.
- [4] S.-G. Chen, M.-H. Chi, J.-Y. Wu, Boundary and interior derivatives estimation for 2D scattered data points, *WSEAS transactions on computers* 5 (2006) 824-829.
- [5] S.-G. Chen, J.-Y. Wu, Discrete conservation laws on curved surfaces, *SIAM Journal on Scientific Computing*, 35(2) (2013) A719-A739.
- [6] U. Clarenz, U. Diewald, M. Rumpf, Anisotropic geometric diffusion in surface processing, In *Proceedings of Viz2000, IEEE Visualization*, (2000) 397-405.
- [7] M. Desbrun, M. Meyer, P. Schroder, A.H. Barr, Implicit fairing of irregular meshes using diffusion and curvature flow, *SIGGRAPH99* (1999) 317-324.
- [8] M. do Carmo, *Differential Geometry of curves and surfaces*, Prentice-Hall International, Inc., London, 1976.
- [9] M. do Carmo, *Riemannian Geometry*, Birkhauser, Boston, 1992
- [10] Colin B. Macdonald, Jeremy Brandman, and Steven J. Ruuth, Solving eigenvalue problems on curved surfaces using the Closest Point Method, *Journal of Computational Physics* 230 (2011) 7944-7956.
- [11] M. Reuter, F.-E. Wolter, N. Peinecke, Laplace-spectra as fingerprints for shape matching, in: *Proceedings of the 2005 ACM symposium on Solid and physical modeling, SPM 05* (2005)101-106.
- [12] B. H. Romeny, *Geometry driven diffusion in computer vision*, Boston, MA, 1994.
- [13] S. J. Ruuth, B. Merriman, A simple embedding method for solving partial differential equations on surfaces, *Journal of Computational Physics*, 227 (2008) 1943-1961.

- [14] G. Kluwer Sapiro, Geometric partial differential equations and image analysis. Cambridge, University Press (2001).
- [15] N. Ray, D. Wang, X.Jiao, and J. Glimm, High-order numerical integration over discrete surfaces, SIAM Journal on Numerical Analysis, 50(6) (2012) 3061-3083.
- [16] Y. Shi, R. Lai, S. Krishna, N. Sicotte, I. Dinov, and A. W. Toga, Anisotropic Laplace-Beltrami eigenmaps: Bridging Reeb graphs and skeletons, in Proc. MMBIA (2008).
- [17] Y. Shi, R. Lai, K. Kern, N. Sicotte, I. Dinov, and A. W. Toga, Harmonic surface mapping with Laplace-Beltrami eigenmaps, in Proc. MICCAI (2008).
- [18] G. Strange and G. Fix, An analysis of the finite element method, Wellesley-Cambridge press 2nd edition, 2008.
- [19] J.-Y. Wu, M.-H. Chi, and S.-G. Chen, A new intrinsic numerical method for PDE on surfaces, International Journal of Computer Mathematics, 89(1) (2012) 54-79.